KeyEngineering Materials Vol. 312 (June 2006) pp. 305-310
Online at http:// www.scientific.net

Critical Behaviour in Concrete Structures and Damage Localization by Acoustic Emission

Alberto Carpinteri[a], Giuseppe Lacidogna[b] and Gianni Niccolini[c]
Politecnico di Torino, Department of Structural Engineering & Geotechnics,
Corso Duca degli Abruzzi 24 – 10129 Torino, Italy
[a]alberto.carpinteri@polito.it, [b]giuseppe.lacidogna@polito.it, [c]gianni.niccolini@polito.it

Keywords: Acoustic emission, Earthquakes, Gutenberg-Richter law, Damage localisation, Concrete structures, Damage mechanics, Crack growth.

Abstract. Extensive research and studies on concrete fracture and failure have shown that concrete should be viewed as a quasi-brittle material having a size-dependent behaviour. Numerous experimental techniques have been employed to evaluate fracture processes, and a number of modelling approaches have been developed to predict fracture behaviour. The non-destructive method based on the *Acoustic Emission* (AE) technique has proved highly effective, especially to check and measure the damage phenomena that take place inside a structure subjected to mechanical loading. In this paper an experimental investigation conducted on concrete and RC structures by means of the AE technique is described. The AE signals reflecting the release of energy taking place during the damage process were recorded and micro-cracking sources were localised by measuring time delays by means of spatially distributed AE sensors.

Introduction

The AE monitoring technique is similar to the one employed in earthquake control, where seismic waves reach the monitoring stations situated on the surface of the earth. Though they take place on very different scales, these two families of phenomena – damage in structural materials and earthquakes in geophysics – are very similar: in either case, in fact, we have a release of elastic energy from sources located inside a medium. Accordingly, the AE technique can be an effective method for monitoring the integrity of large-sized structures, such as buildings and other constructions, by means of a limited number of sensors.

Another similarity between complex seismic phenomena and damage processes in structures, as assessed by means of the AE technique, is provided by the statistical distribution of earthquakes: high magnitude earthquakes, in fact, are less frequent than lighter quakes, a phenomenon that is quantified by the Gutenberg-Richter (GR) law [1]. By applying this law to AE analysis, a statistical correlation between the number of AE events (N) and signal amplitude has been worked out. In this manner, we can gain a better understanding of the relationship between microstructural events and macroscopic behaviour and we are in a better position to formulate predictive models, either about laboratory scale effects or full-size structural performance and reliability.

In AE monitoring, piezoelectric (PZT) sensors are used, thereby exploiting the capacity of certain crystals to produce electric signals whenever they are subjected to a mechanical stress. The adopted equipment in this investigation consists of many units USAM®, that can be synchronized for multi-channel data processing. Each unit contains a preamplified wideband PZT sensor sensitive at the frequency range between 100kHz and 500kHz. The most relevant parameters acquired from the signals (arrival time, amplitude, duration, and number of oscillations) are stored in the USAMs memory and then downloaded to a PC for a multi-channel data processing. From this elaboration microcracks localisation is performed and the condition of the specimen can be determined.

AE Frequency-Magnitude Statistics

Along the lines of the earthquake seismology [1], the magnitude in terms of AE technique is defined as follows:

$$m = Log_{10} A_{\max} + f(r), \tag{1}$$

where $A_{\max}$ is the signal amplitude, measured in microvolts, while $f(r)$ is a correction taking in account that the amplitude is a decreasing function of the distance r between the source and the sensor. According to Uomoto [2], for large-sized structures, the amplitude reduction for AE signals in concrete is $f(r) = k\,r$, where r is measured in meters and k is equal to five magnitudes per meter.

In seismology, earthquakes of larger magnitude occur less frequently than earthquakes of smaller magnitude. This fact can be quantified in terms of a magnitude-frequency relation, proposed by Gutenberg and Richter in an empirical way:

$$Log_{10} N(\geq m) = a - bm, \text{ or } N(\geq m) = 10^{\,a-bm}, \tag{2}$$

where N is the cumulative number of earthquakes with magnitude $\geq m$ in a specified area and over a specified time span, and b and a are positive constants varying from region to region.

The GR relationship has been tested successfully in the acoustic emission field to study the scaling of the ''amplitude distribution'' of AE waves [4,5]: this approach substantiates the similarity between the damage process in a structure and the seismic activity in a region of the Earth and, at the same time, it widens the scope of the GR relationship. From Eq. (2), we find that the b-value is the negative gradient of the log-linear AE frequency-magnitude diagram and hence it represents the slope of the amplitude distribution. The b-value changes systematically with the different stages of fracture growth [4,5], and hence it can be used to estimate the development of fracture process.

Damage Size-Scaling. The aim is to establish a theoretical basis for taking $b_{\min} = 1$, as observed both in AE laboratory tests and in tests performed on full sized engineering structures [5-8]. By analogy with earthquakes, the AE damage *size-scaling* entails the validity of the relationship:

$$N(\geq L) = c\,L^{-2b}, \tag{3}$$

where N is the cumulative number of AE events generated by source defects with a characteristic linear dimension $\geq L$; c is the total number of AE events and $D = 2b$ the fractal dimension of the damaged domain [3,9]. The cumulative distribution (3) is substantially identical to the cumulative distribution proposed by Carpinteri [6-8], which gives the probability of a defect with size $\geq L$ being present in a body:

$$P(\geq L) \propto L^{-\gamma}, \tag{4}$$

Therefore, the number of defects with size $\geq L$ is:

$$N^{*}(\geq L) = N_{tot}\, L^{-\gamma}, \tag{5}$$

where γ is an exponent measuring the degree of disorder, i.e. the scatter in the defect size distribution, and N_{tot} is the total number of defects in the body.

Equating distributions (3) and (5) it is found that: $2b = \gamma$. At the collapse, the size of the maximum defect is proportional to the characteristic size of the structure. As shown in [6-8], the related cumulative defect size distribution (referred to as self-similarity distribution) is characterized by the exponent $\gamma = 2$, which corresponds to $b = 1$. Carpinteri [6-8] has also shown that $\gamma = 2$ is a lower limit which corresponds to the minimum values $b = 1$ observed experimentally when the load bearing capacity of a structural member has been exhausted.

Damage Time-Scaling. The authors have also shown that energy release W, as measured with the AE technique during the damaging process, follows this *time-scaling* law [10]:

$$W(t) \propto N(t) \propto t^{\beta_t}, \tag{6}$$

where t is the monitoring time, N is the total number of AE events relating to a certain predetermined magnitude, m_0, and taking place over a certain time period, and β_t stands for the time-scaling exponent of the energy released.

Eq. (6) describes – as does Omori's law [3], but in simpler, more intuitive terms – the sequences of foreshocks and aftershocks characterising the failure of a structural member during a loading test. By working out the β_t exponent from the data obtained during each observation period, we can make a prediction as to the stability of a structure. If $\beta_t < 1$, the damaging process slows down, because energy dissipation tends to decrease; if $\beta_t > 1$ the process becomes unstable, and if $\beta_t \cong 1$ the process is metastable, i.e., though it evolves linearly over time, it can reach either stability or instability conditions indifferently. By introducing Eq. (2) into Eq. (6) we get the experimental relationship between the b-value of the GR law and the time-scaling exponent β_t:

$$Log_{10}N(\geq m_0,t) = a(t) - b(t)m_0 \propto \beta_t Log_{10}t \text{ , or } N(\geq m_0,t) = 10^{a(t)-b(t)m_0} \propto t^{\beta_t} . \quad (7)$$

During the application of the load to a structural member, whether on a laboratory or a full size scale, the critical condition (mainshock) can be identified as the condition in which AE signal amplitude is greatest. Accordingly, from Eq. (7) it is possible to determine the $a(t)$, $b(t)$ time-dependent coefficients and the β_t parameter for each interval in the time succession analysed. In general, we find that in the sequences of signals preceding the critical condition (foreshock) $\beta_t > 1$, and in those that follow (aftershock) $\beta_t < 1$. The b-value parameter, instead, in keeping with Carpinteri's observation [6-8], decreases continuously until it reaches $b_{min} = 1$ at the end of the loading process.

Experimental observations

***In Situ* Retrofitted RC Beam Test.** Utilizing the AE technique, we have monitored and analysed a retrofitted RC beam with non-rectangular cross-section (Fig. 1). To improve its load carrying capacity and attenuate the effects of microcracking, the beam was reinforced externally with FRP sheets after the prior removal of the existing overload [11]. Then, an *in-situ* loading test of the retrofitted beam was carried out.

The entire loading test lasted approximately 3 hours. During the test, five transducers (S_i) were applied to one of the lateral faces of the beam. The AE source points were determined and are shown in Fig. 1(c) with black dots. In the loading range considered, micro-slips between the FRP sheets and concrete were not high enough to cause delamination. AE transducers, in fact, detected the onset of debonding only. The time evolution of the AE counting numbers, as detected by the AE transducers, is shown in Fig. 1(d). Transducers 3 and 4 were close to flexural cracks and began to detect AE events from the beginning of the loading test. At the end of the test, they had detected the highest number of AE, followed by transducers 1 and 2, which were close to the beam supports.

This result is in agreement with the typical progression of cracking and collapse in retrofitted beams. Flexural cracks propagate upwards as loading progresses, but remain very narrow throughout the loading history. Delamination of the FRP sheets together with a thin layer of concrete takes place only when shear cracks develop in the proximity of the supports.

In addition to the crack localisation, the cumulative number of AE events with magnitudes greater than m as a function of m, was plotted on a semi-logarithmic scale. The final determination for the magnitude of an AE event is based on the average value of the results recorded by all the sensors. The reading of a single sensor is found using Eq. (1). From Fig. 1(e) a good agreement with the GR relationship is observed: the b-value is around to 1.470.

Three-Point Bending Test. The behaviour of a specimen subject to a three-point bending test was investigated. To determine the fracture process zone, AE generation was monitored. The specimen was a prism measuring 8 x15 x 70 cm^3, with a central 5 cm notch cut into it beforehand to ensure a centre crack. Five AE transducers were fitted to the specimen at points shown in Fig. 2(a). During the loading test, the source location procedure was successfully applied to identify the fracture process zone, as shown in Fig. 2(a). Nucleation in the fracture process zone might be correlated with the AE clusters zone, and AE clusters are seen to propagate with increasing load [12]. The load

vs. time curve for the specimen, characterizing the AE activity, is shown in Fig. 2(b). In order to assess the ability of AE the technique to monitor the microscopic damages occurring inside the material and obtain information about the fracture processes, the load-time diagram, plotted for each second of the testing period, was broken down into three stages: a first stage (t_0, t_1) extending from the initial time to peak load, a second stage (t_1, t_2) going from peak load to the mainshock, and a third stage (t_2, t_f) going from the mainshock to the end of the process. In accordance with the GR law, *b*-values are shown for each stage in Fig. 2(c). In this case too the *b*-values are seen to be in good agreement with the GR law: they range from 1.4939 to 1.1154. The minimum value is obtained in the softening branch of the load-time curve, and it is very close to 1, as predicted in [6-8].

Concrete Specimen in Compression. Laboratory tests also analysed the behaviour of cylindrical concrete specimens in compression [10]. One of the 59 mm diameter specimens, with a height/diameter ratio $h/d = 2$, is shown in Fig. 3(a). The compression test were performed in displacement control, by imposing a constant rate of displacement of the upper loading platen. A displacement rate equal to 4×10^{-4} mm/s was adopted to obtain a very slow crack growth. Compressive load vs. time, cumulated event number, and event rate (for each second of the testing period) are depicted in Fig. 3(b). Also in this case, the load-time diagram was subdivided into three stages. The *b*-values obtained for each stage are shown in Fig. 3(c); they range from 1.6363 to 1.1981. The minimum value, very close to 1, was again obtained in the softening branch of the load-time curve. Finally, for the three loading stages, Fig. 3(d) gives the values of the β_t parameter. The values, between 1.626 and 0.583, were determined by best fitting the cumulating count of the AE events divided by the total count for each loading stage. These results confirm that during the sequences of signals preceding the critical condition (foreshock), $\beta_t > 1$, whereas during the sequences following the critical condition (aftershock), $\beta_t < 1$, energy dissipation having been exhausted. It should be noted that a comparative reading of the *b*-value and β_t parameter makes it possible to assess the evolution of the entire loading process: the β_t parameters, in fact, have a *predictive* function relative to the reaching of the critical condition, whereas *b*-values have a *descriptive* function relative to the damage level reached. Correlation between size scaling on specimen dimension and AE activity are clearly explained in [10].

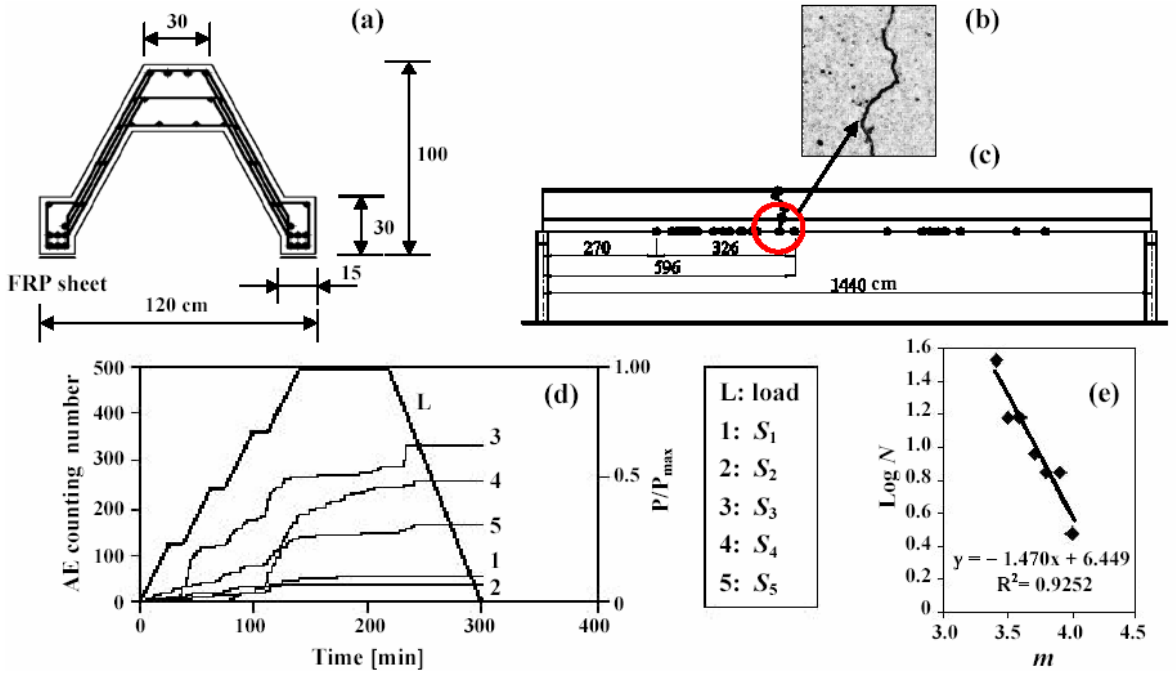

Fig. 1. *In situ* retrofitted RC beam test. (a) Scheme of the beam cross-section. (b) Photo of a flexural crack in between transducers 3 and 4 (using an optical microscopy with magnification 100X). (c) Scheme of the beam indicating localized AE sources. (d) AE counting number for each sensor S_i during the loading test. (e) *b*-value during the loading test.

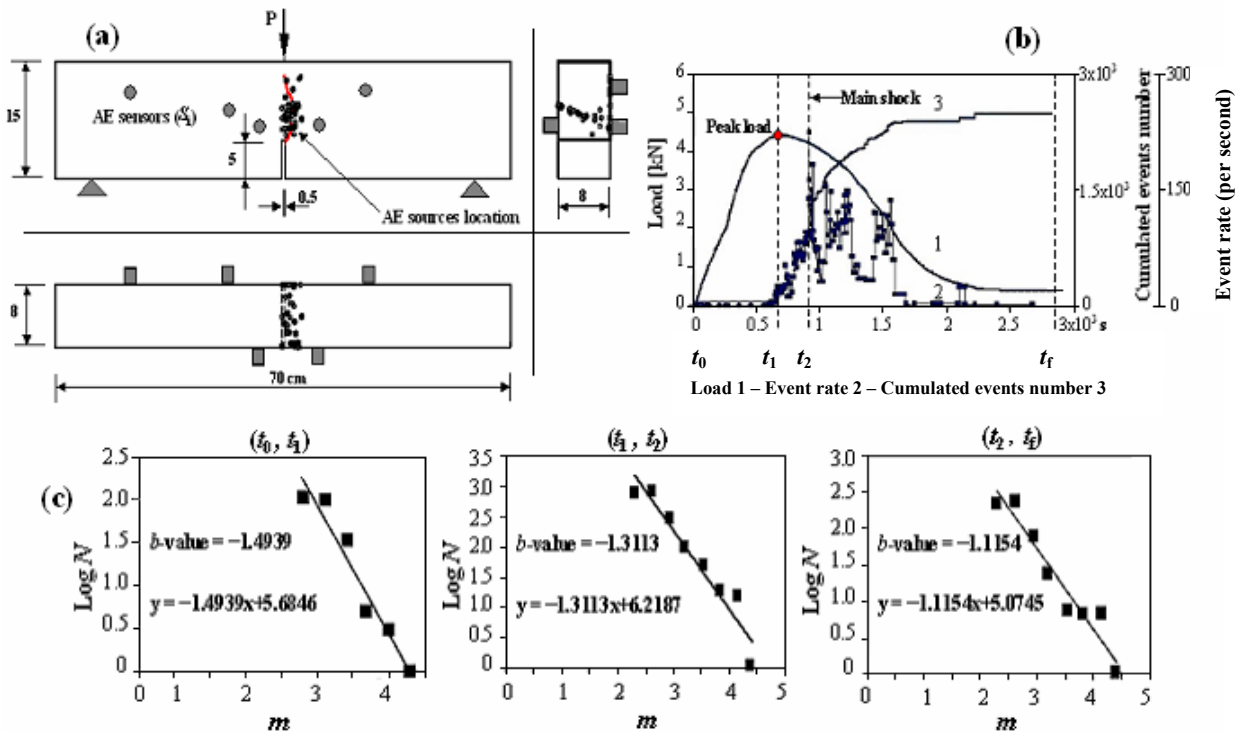

Fig. 2. Three bending point test. (a) Identification of the fracture process zone. (b) Load vs. time curve and AE activity. (c) *b*-values during the loading test.

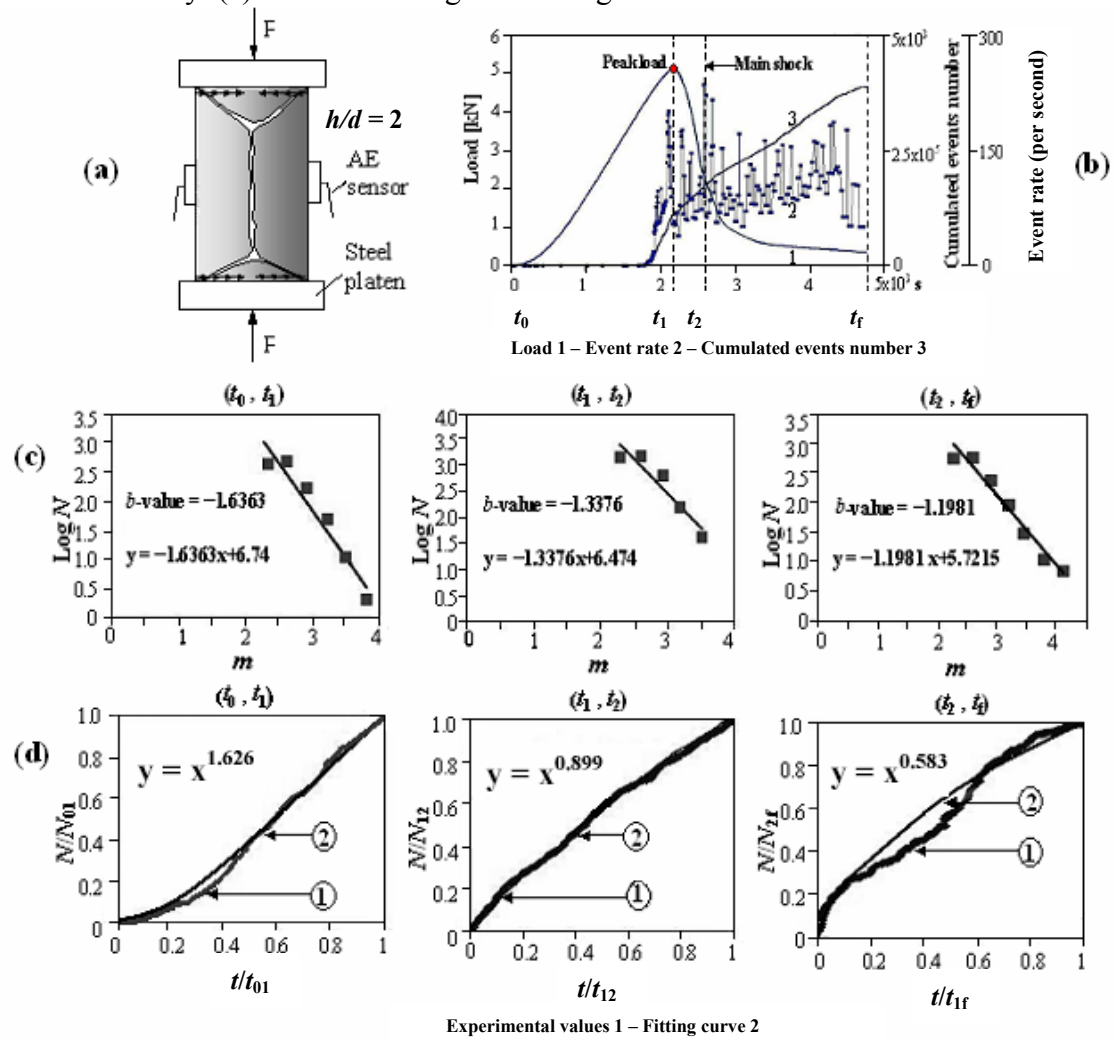

Fig. 3. Cylindrical concrete specimen in compression. (a) Testing set-up. (b) Load vs. time curve and AE activity. (c) *b*-values during the loading test. (d) Variation in β_t parameter during the test.

Conclusions

The acoustic emission (AE) technique has the potential for performing an effective monitoring of the integrity of large-sized structures, such as Civil Engineering structures, by means of a limited number of sensors. By applying the AE technique to structural members monitored during the damaging process, a statistical correlation between the number of AE events and their amplitude was established by quantifying the *b*-value for each loading stage; the time-scaling was determined through the β_t parameter. From the values of these two coefficients we can get a better understanding of the relationship between microstructural events and macroscopic behaviour and we are in a better position to formulate predictive models, either about laboratory scale-effects or full-size structural performance and reliability.

Acknowledgements

Support of the Ministry of University and Scientific Research (MIUR) and of the European Union (EU) is gratefully acknowledged.

References

[1] C.F. Richter: *Elementary Seismology*. W.H. Freeman and Company, San Francisco and London, 1958.

[2] T. Uomoto: Application of acoustic emission to the field of concrete engineering. *Journal of Acoustic Emission*, Vol. 6 (1987), p. 137-144.

[3] J.B. Rundle, D.L. Turcotte, R. Shcherbakov, W. Klein, C. Sammis: Statistical physics approach to understanding the multiscale dynamics of earthquake fault systems. *Reviews of Geophysics*, Vol. 41 (2003), p. 1-30.

[4] P.R. Sammonds, P.G. Meredith, S.A.F. Murrel, I.G. Main: Modelling the damage evolution in rock containing porefluid by acoustic emission. *Proc. of Eurock'94*, Balkerna, Rotterdam, The Netherlands (1994).

[5] S. Colombo, I.G. Main, M.C. Forde: Assessing damage of reinforced concrete beam using ''b-value'' analysis of acoustic emission signals. *Journal of Materials in Civil Engineering* ASCE, Vol. 15 (2003), p. 280-286.

[6] A. Carpinteri: *Mechanical Damage and Crack Growth in Concrete: Plastic Collapse to Brittle Fracture.* Martinus Nijhoff Publishers, Dordrecht, 1986.

[7] A. Carpinteri: Decrease of apparent tensile and bending strength with specimen size: two different explanations based on fracture mechanics. *International Journal of Solids and Structures,* Vol. 25 (1989), 407-429.

[8] A. Carpinteri: Scaling laws and renormalization groups for strength and toughness of disordered materials. *International Journal of solids and structures*, Vol. 31 (1994), p. 291-302.

[9] K. Aki, P.G. Richards: *Quantitative Seismology: Theory and Methods*. W.H. Freeman & Co., New York, 1980.

[10] A. Carpinteri, G. Lacidogna, N. Pugno: Damage diagnosis and life-time assessment of concrete and masonry structures by an acoustic emission technique. *Proc. of 5th Intern. Conf. on Fracture Mechanics of Concrete and Concrete Structures* (FraMCos-5), Vail, Colorado-USA, pp. 31-40. Eds. V. C. Li, C. K. Y. Leung, K. J. Willam, S. L. Billington, 2004.

[11] A. Carpinteri, G. Lacidogna, M. Paggi, N. Pugno: Acoustic emission monitoring and numerical modeling of a FRP-strengthened concrete structure. *Intern. Conf. on Concrete Repair, Rehabilitation and Retrofitting* (ICCRRR 2005), Cape Town, South Africa, 2005.

[12] M. Ohtsu: The history and development of acoustic emission in concrete engineering. *Magazine of Concrete Research*, Vol. 48 (1996), p. 321-330.